CCD STAR TRACKERS*

W. C. Goss
Jet Propulsion Laboratory
Pasadena, California

This paper presents an overview of current activities at JPL directed toward the application of CCDs to star trackers and star mappers. The advantages and disadvantages of silicon CCD star trackers are compared with those of image dissector star trackers. It is concluded that although the image dissector provides somewhat greater sensitivity for tracking single stars, the CCD has adequate sensitivity for most single star tracking tasks and is distinctly superior in multiple star tracking or mapping applications. In addition, the CCD has major advantages in terms of size, weight, stability and growth potential.

The signal and noise figures of several current CCD configurations are discussed. The basic structure of the required signal processing is described, and it is shown that resolution in excess of the number of CCD elements may be had by interpolation.

CCD star trackers and star mappers now under development at JPL will utilize microprocessors for their signal processing. Some major advantages of the microprocessor approach are discussed and include the ability to use data which is in an interlaced field format.

*This paper presents the results of one phase of research carried out at the Jet Propulsion Laboratory, California Institute of Technology, under Contract No. NAS 7-100, sponsored by the National Aeronautics and Space Administration.

I. INTRODUCTION

JPL currently has two tasks funded by the NASA Office of Aeronautics and Space Technology to develop CCD star reference trackers for spacecraft and payload stabilization. One of these tasks is directed toward providing a single-axis star tracker which will be used for roll axis stabilization of Mariner-type spacecraft on missions subsequent to Mariner Jupiter-Saturn 1977. The other task is to develop a star pattern sensor having the capability of tracking ten stars simultaneously, providing two-axis coordinates and magnitude data for each and providing a video signal for display of the star field on a television monitor. The intended application is astronomer-supervised acquisition of infrared target bodies by the Shuttle Infrared Target Facility, a Shuttle payload now in the definition phase.

This paper presents the rationale for the choice of a charge-coupled image sensor for these tasks, discusses CCD star image signal processing techniques and outlines expected performance parameters.

II. IMAGE DISSECTORS VS. CCDs

Image dissectors have been in wide usage for more than a decade as the preferred star magnitude and position sensing elements in star trackers. Image dissectors are, very simply, photomultiplier tubes with an electron imaging and electron deflection section located between the photocathode and a sampling aperture which is at the entrance to the electron multiplier section. Image dissectors provide optical signal modulation and field of view gimballing without the use of moving parts.

Image dissectors can be almost completely signal shot noise limited. The large and comparatively noise-free gain in the multiplier section reduces the effect of subsequent leakage currents and amplifier noise contributions to an insignificant level. Modern photocathodes have thermal emissions of only a few electrons per second or less for typical image dissector electron aperture areas. Pulse height discrimination photon counting techniques exclude the majority of electrons thermally emitted within the multiplier structure and can ignore the multiplier gain distribution function. In the absence of a significant sky background or ambient radiation field, an image dissector can reliably detect a few photoelectron events per sampling period (Ref. 1).

However, image dissectors have a number of disadvantageous characteristics which have encouraged designers to consider alternatives; these characteristics principally include the non-storage feature which heavily penalizes sensitivity under multiple target or full frame search conditions, variable and unsymmetrical magnification across the field which necessitates elaborate calibration for precise offset pointing, fatigue and damage susceptibility of the photocathodes, relatively high weight and power demand, use of high voltages, fragility, susceptibility to magnetic fields and cost, to name a few.

Silicon photodiode or photovoltaic detectors have appeared attractive for some applications by contrast because of their low cost, small size, rugged construction, stability, insensitivity to magnetic fields and ability to operate at voltage levels compatible with microcircuits. Solid-state star trackers have been built and flown using silicon detectors despite their limited fields of view, relatively poor sensitivity, and inability to electronically gimbal or provide accurate star position information except in a very limited region about null.

Silicon CCD sensors now provide the designer with a superior alternative which exhibits all the strong points of the silicon detector, has few of its weaknesses and provides valuable capabilities not obtainable from either the image dissector or the silicon sensor. The minute area of the individual CCD elements along with the charge storage capability and the broad-band high quantum efficiency silicon response combine to produce an ultimate sensitivity, when cooled to moderately low temperatures, within one stellar magnitude or less of the threshold for an ideal image dissector, all other factors remaining the same. This number can be arrived at by comparing the response of silicon and an S-20 photocathode -- a ratio of typically 8/1 for a relatively hot type F star (Ref. 2) -- and the signal level at unity signal-to-noise ratio for the two detectors. Those numbers are typically 3 electrons per interval for an image dissector and presently about 150 electrons per element for a CCD. Including a duty cycle factor of 1/2 for the image dissector modulation, a threshold stellar irradiation ratio of 3 results, corresponding to 1.2 stellar magnitudes.

This slim margin in favor of the image dissector vanishes decisively if a cooler star is the target, or if the dissector is required to track multiple

targets or to scan the full field in search. Unlike the image dissector, the charge storage and full field readout features of the CCD make its star magnitude threshold independent of the number of targets.

A further advantage of the discrete detector configuration is that the sensor is relatively insensitive to nonsaturating levels of stray light or sky background. The only illumination which can interfere with the star target signals is that illumination which is intercepted by the same elements upon which the star is imaged. Background level subtraction in the signal processing can then remove the mean value of the interfering illumination. Fixed pattern variations and shot noise will remain.

Several problems are inherent in the use of CCDs for star trackers that are not encountered using image dissectors. Room temperature average dark charge generation rates are typically so high as to fill the CCD wells in a few seconds, and individual high dark charge elements may have generation rates several times the mean value. Cooling to moderately low temperatures, for example to -40°, will be necessary to reduce the dark charge and so provide a usable dynamic range. Experience at JPL with other space instruments, for example, the Mars Atmospheric Water Detector, shows that packages may be reliably cooled to even lower temperatures by utilizing passive radiation to space.

Several signal processing complexities arise because of the discrete detector array structure. A star image will not in general fall upon a single element at a time. Even a point image will often be quadrisected at the common corner of four cells. A very small image might, in fact, "fall into the crack" between elements if the CCD were an interline transfer device. For these reasons as well as others, it will often be useful to work with an image point spread function measuring two or more elements in width and to measure star magnitude by summing the signal from a small group of adjacent elements large enough to include all the signal from a star image.

A related problem is that the number of image elements now available in CCDs is smaller than the incremental resolution needed in most star tracker applications. The largest imaging CCD array commercially available at this time is RCA's Big Sid, a surface-channel device having 256 × 312 elements. Buried-channel arrays of about 400 × 400 elements are being developed by

Texas Instruments and Fairchild. Star tracker requirements frequently demand 1000 or more resolution elements across the field in order to provide offset pointing capability. Present CCD fabrication techniques can generate cell structures with adequate geometric accuracy, and as will be discussed further in this paper, simple interpolation techniques may be used to locate the centroid of an extended star image to within a small fraction of a pixel. These signal processing techniques require substantial memory capacity and logic capability since signals from as many as nine separate image elements must be processed in several ways to derive star magnitude and an interpolated image centroid position, and the signals will not all be located consecutively in the data stream. Use of an interlaced CCD data stream would, in fact, produce part of the data in one field and the rest in the other.

Signal processing is operationally much more complex than for an image dissector star tracker, which simply phase demodulates to obtain star position within the scan width and obtains a direct measure of star magnitude from the multiplier current or voltage. Signal processing circuitry then could be expected to be complex by comparison. Although this computational task is relatively complex in hardware, it is relatively simple in software, and use of a microprocessor provides at once a functional simplicity and a great flexibility in altering tracker characteristics to meet a variety of functional requirements.

A final consideration in the tradeoff between image dissectors and CCDs is the question of present and future availability. The image dissector is a mature device with fairly consistent and predictable characteristics, and commercial devices are readily available at prices of a few thousand dollars. The market is relatively small. This comment will probably still be correct 10 years from now. CCD devices, on the other hand, are still developing very rapidly and have a large growth potential. Very few devices are available on the commercial market today, and they must be regarded as forerunners of more capable devices yet to come. A very large commercial market is expected to develop, and price competition will be strong. In 10 years, if we should apply the experience of the integrated circuit industry, the CCD imagers which are available today will amost certainly be obsolete and unavailable. More sophisticated and more reliable devices will have replaced them at prices perhaps in the tens of dollars.

III. CCD SIGNAL CHARACTERISTICS

If we assume that the star image signal charges which are generated in adjacent elements are reconstituted by the signal processing circuits into a total value representing the entire image, then the detector response to a star can be characterized by

$$Q_S = \frac{aA\Delta T}{q} \int R(\lambda)S(\lambda)\, d\lambda \qquad (1)$$

where

Q_S = star signal in electrons
a = ratio, detector element area to unit cell area
A = objective lens area
ΔT = charge integration time
q = electronic charge
$R(\lambda)$ = detector response, amp/watt
$S(\lambda)$ = star irradiation spectral power density

Figure 1 illustrates the normalized spectral energy density of α-Carinae (Canopus) (Ref. 3), a type F star having an effective black-body temperature of 7000° Kelvin, and for comparison, spectral response curves for two differently structured CCDs. The lower curve, for the Fairchild CCD 201, has a peak response of nearly 0.3 amp/watt and effective short and long wavelength cutoffs of 0.45 and 1.1 microns. The upper curve plots spectral response measured by Texas Instruments on a promising backside illuminated and thinned device now under development for JPL. Peak response is 0.4 amp/watt, with a long wavelength cutoff of 0.1 micron and a short wavelength cutoff which was not measured but must be well below 0.4 micron.

Using the data of Figure 1 and a structural shadowing factor a = 0.5 for the Fairchild device, we obtain from Equation (1) a charge generation rate of 1.26×10^6 electrons/second for each cm^2 of objective lens area. A similar calculation for the Texas Instruments device, assuming a = 1.0, yields a generation rate of 7.1×10^6. It is of interest to note that this response is slightly greater than the value tabulated in Ref. 2 for the silicon detector response to Canopus.

IV. NOISE CHARACTERISTICS

Noise sources in CCDs which compete with the detected signal fall into several categories. Thermal generation of carriers within the bulk silicon and at the interfaces provides a temperature-dependent dark current that supplies, at best, a uniform background charge level in the storage elements and, at worst, a pronounced fixed pattern of spikes. Statistical variations in signal plus dark current electrons introduce the familiar shot noise. Transfer losses introduce highly correlated errors. Clocking and reset waveforms appear at the output, introducing coherent noise. Surface state trapping introduces yet another noise factor in surface-channel CCDs.

Dark current is a limiting factor in several ways. The accumulated charge can simply fill the potential wells and leave no room for storage of photo-generated signals. Lower-level uniform background charges may be subtracted by the signal processing circuits; however, shot noise proportional to the square root of the number of thermal charges in each element remains. Finally, individual high dark current elements produce signals which would be difficult to differentiate from star signals if of large enough amplitude.

Room temperature dark current generation rates for typical silicon diffusions, as used in buried channels, should be approximately 3 na/cm^2 (Ref. 4), or approximately 1.2×10^5 electrons per element per second, assuming element dimensions of 25 microns on a side. Many have much larger average rates, however; 10 na/cm^2 are not unusual with some individual elements having rates as much as 6 na/cm^2 above the mean. These high dark current elements would appear as bright stars and would seriously interfere with the star tracker operation. Fortunately, moderate cooling should reduce the accumulated dark charge to a level below the minimum detectable signal level, taken earlier to be 150 electrons. Data reported by Fairchild (Ref. 5) indicates that operation at -40° will reduce dark current rates by 600 times below room temperature rates. Assuming a 1.1-second integration time, the dark charge collected will be 100 electrons or less.

The principal noise constituents, then, assuming framing rates of 10 per second or greater, can be expected to be clocking and reset noise at low light levels and shot noise at signal levels higher than about 4% of saturation.

Improvements made in reducing clock waveform coupling and in developing low-noise output amplifiers will be directly translatable into an improved small signal sensitivity, although additional cooling might be required to realize the gain.

Taking 150 electrons as our threshold detectable signal, multiplying by three to account for summing nine total elements and multiplying again by four to achieve a reasonable signal-to-noise ratio, we decide on a criterion for threshold detection of stars of N_t = 1800 electrons accumulated during a single integration time. Extrapolating signal response for stars of magnitudes other than our example in Figure 1,

$$Q(m) = Q_S(2.512)^{(m_o - m)} \tag{2}$$

and, substituting into Equation (1), we can write a scaling expression for the diameter of lens which is required in order to detect a star of a given magnitude:

$$d = \left[\frac{4qN_t(2.512)^m}{(2.512)^{m_o} a \pi \Delta T \int R(\lambda)S(\lambda)\cdot d} \right]^{1/2} \tag{3}$$

This expression is plotted in Figure 2 for the Fairchild and Texas Instruments CCDs. Note that a 1-cm-diameter lens, for example, will collect light enough to see a magnitude 3 1/2 star with the Fairchild device and a magnitude 5 1/2 star with the Texas Instruments CCD.

V. INTERPOLATION

The previous discussion has explored star detection capabilities of the Fairchild CCD image sensor, which is commercially available now, and of a Texas Instruments sensor currently under development. The conclusion is that these devices have very useful star detection capabilities. However, detection and identification of a guide star are only prerequisites to the principal task of generating relative star position coordinates with adequate accuracy and resolution.

As noted earlier, present-day CCDs have fewer image elements than the total number of resolution elements often required. The following discussion will address the subject of an interpolation providing adequate accuracy for the present requirements, yet simple enough to be built into a flight instrument.

We will consider first CCDs which are organized with vertical transfer, and then discuss interpolation with devices which have interline transfer.

We will assume that charge is not lost between elements, and that the image point spread function is symmetrical and one or more element-widths in diameter so that charge levels in adjacent elements may be compared to determine the location of the image center. We will not consider a detector point spread function apart from the image spread function. Assume first that we have an arbitrary image point spread function

$$I = f_1(x, y)$$

If we can make detailed measurements of the function, we may obtain the line spread functions in x and y, I(x) and I(y), by integrating over the image width in the other direction. We may then calculate centroids along both axes; for example,

$$X_c = \frac{\int xI(x)\, dx}{\int I(x)\, dx} \tag{4}$$

Figure 3 illustrates how the point spread function might look to a CCD imager. The continuous point spread function has been integrated in steps over the sub-interval areas represented by the CCD elements. We can still form line spread functions by summing in one dimension, as shown in Figure 4; however, accurate calculation of centroids is frustrated by uncertainty as to the shape of the image function within the element boundaries. The difficulty is resolved if we have a priori knowledge of the shape of the line spread function, and calculation becomes appealingly simple if the line spread function is rectangular.

If we have an image of width greater than one element and less than two, the line spread function will be fully defined by three successive elements, which we designate F_{k-1}, F_k, and F_{k+1}, and the x-direction centroid position will be

$$X_c = \frac{F_{k+1} - F_{k-1}}{2F_k}, \quad \text{for } -0.5 \leq x_c \leq 0.5 \tag{5}$$

This expression is exact for a rectangular line spread function and very nearly so for some reasonable approximations. A point spread function of the form

$$I(r) = a + br^2, \quad r \leq 1 \tag{6}$$

can, in principle, be interpolated by Equation (5) to an accuracy of 1%.

Point spread functions of that form can be generated by several techniques, including defocusing the image formed by a folded mirror objective. Even line spread functions far removed from the rectangular shape are reasonably well interpolated by Equation (5). Figure 5 illustrates the interpolation accuracy of an image having a Gaussian spread function. Best results are obtained for the largest image, and indications are that the optimum size may be even larger. From smallest to largest, the maximum errors are 14.6%, 11.6% and 8.3%. A 0.6% step is observed to occur at the ends of the range for the largest image if the output is not rescaled.

Interpolation with devices having interline transfer is also feasible even though the interline transfer registers are opaque and strips of the image are lost. A variety of techniques are available; however, a calculationally simple approach similar to the one just outlined for vertical transfer devices will be described. We consider a symmetrical triangular line spread function of approximately 2 1/2 unit cell widths. We construct the sides of the triangle

from the measured element signals and calculate the intersection point. The centroid then will be

$$X_c = \frac{F_{k+1} - F_K}{F_{k-1} + F_k + F_{k+1}}, \quad -0.5 \leq x_c \leq 0.5 \tag{7}$$

This expression is not exact for a triangular line spread function; a maximum positional error of about 6% results. A Gaussian line spread function, which results from a Gaussian point spread function, is a fairly good approximation to a triangular form, and a maximum error of 8% results, as illustrated in Figure 6. The signal summation $F_{k-1} + F_k + F_{k+1}$ is constant to within about 3% over the full range of image positions.

VI. SUMMARY

In summary, the technical tradeoff between image dissectors and CCDs for star tracker applications provides a clear picture of major performance and configurational advantages in favor of CCDs, although the image dissector is somewhat more sensitive for tracking single hot stars. The outstanding disadvantages of the CCD are that it requires cooling and that the signal processing is more complex than for an image dissector. A close look indicates that these are not serious problems; passive radiation to space can provide the necessary cooling, and the signal processing, on close inspection, proves to be difficult for hardwired processing but straightforward for logical processing, as with a microprocessor. The CCD technology is immature at this time, and only a very limited selection of devices is available. Finally, measurement of the image position on an array by interpolation to an accuracy of 1/10 of an element appears feasible for both types of CCDs.

REFERENCES

1. E. H. Eberhardt, "Multiplier Phototubes as Quantum Counters," Applied Optics, Volume 6, No. 1, 1967.

2. F. F. Forbes and R. I. Mitchell, "Stellar Photometric Data For Six Different Photocathode Materials and the Silicon Detector," Communications of the Lunar and Planetary Laboratory # 141, 1968.

3. R. H. Norton, The Absolute Spectral-Energy Distribution of Canopus, JPL Technical Report 32-641, August 15, 1964.

4. Charge Coupled Device Image Sensor Study, Final Technical Report, JPL Contract 953674, Fairchild Camera & Instrument Corporation, February 1974.

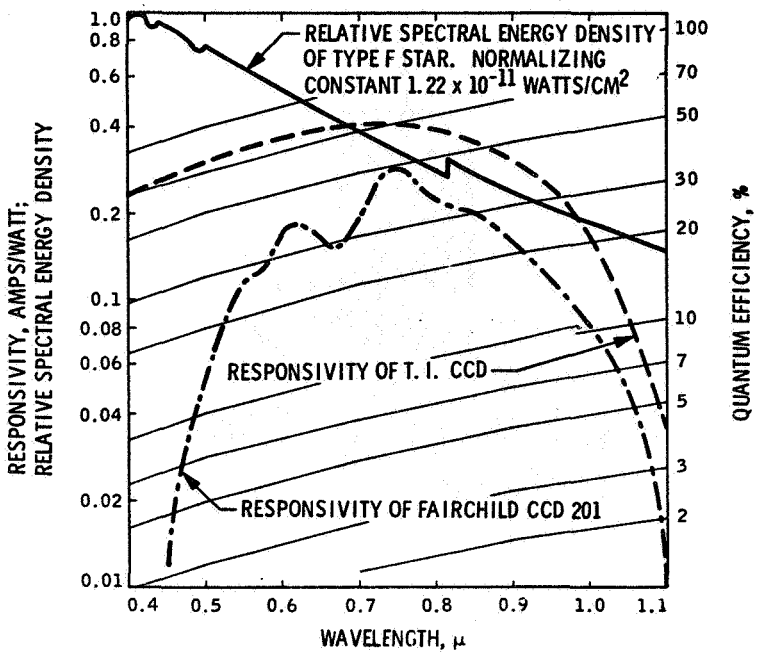

Figure 1. Typical star source and CCD response characteristics

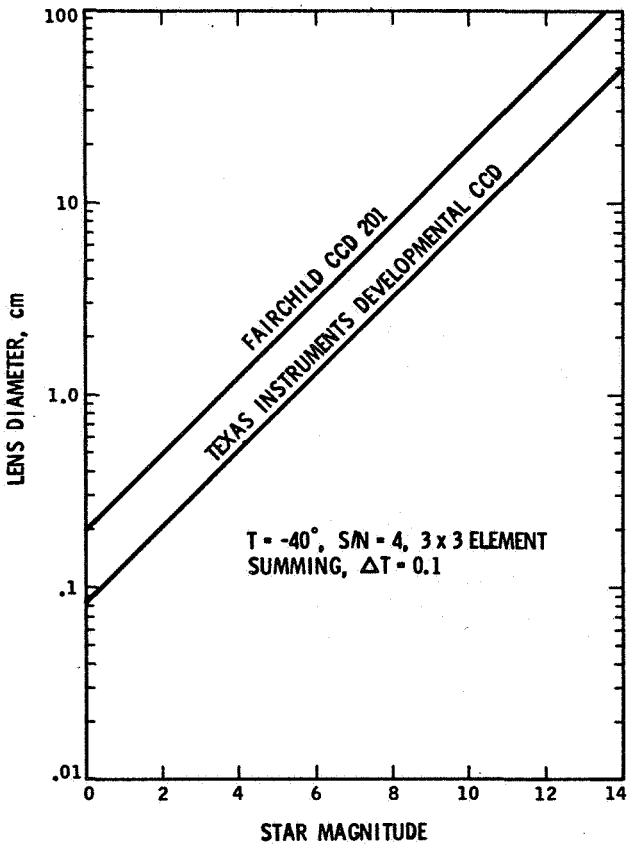

Figure 2. Star detection thresholds

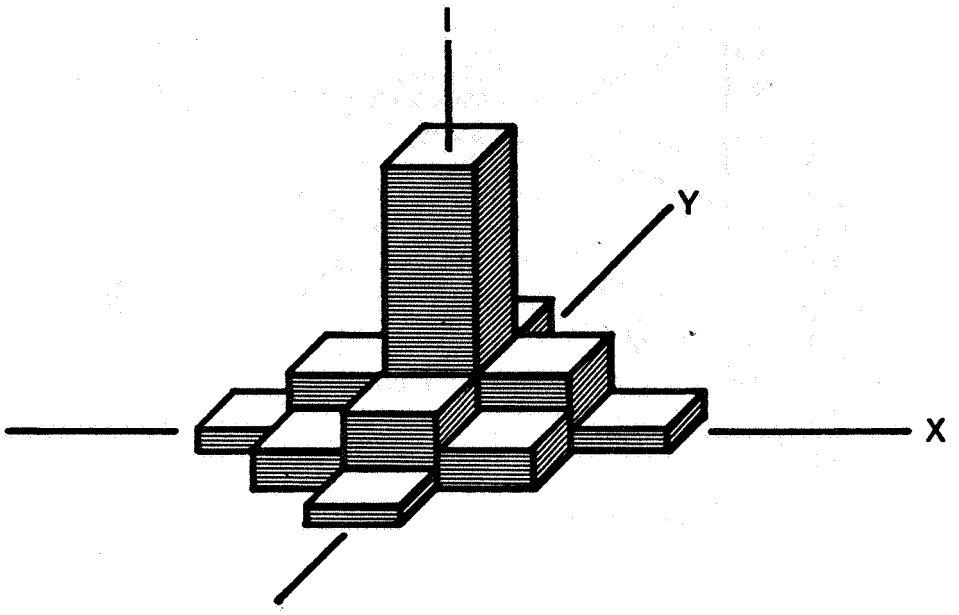

Figure 3. Image point spread function as seen by CCD array

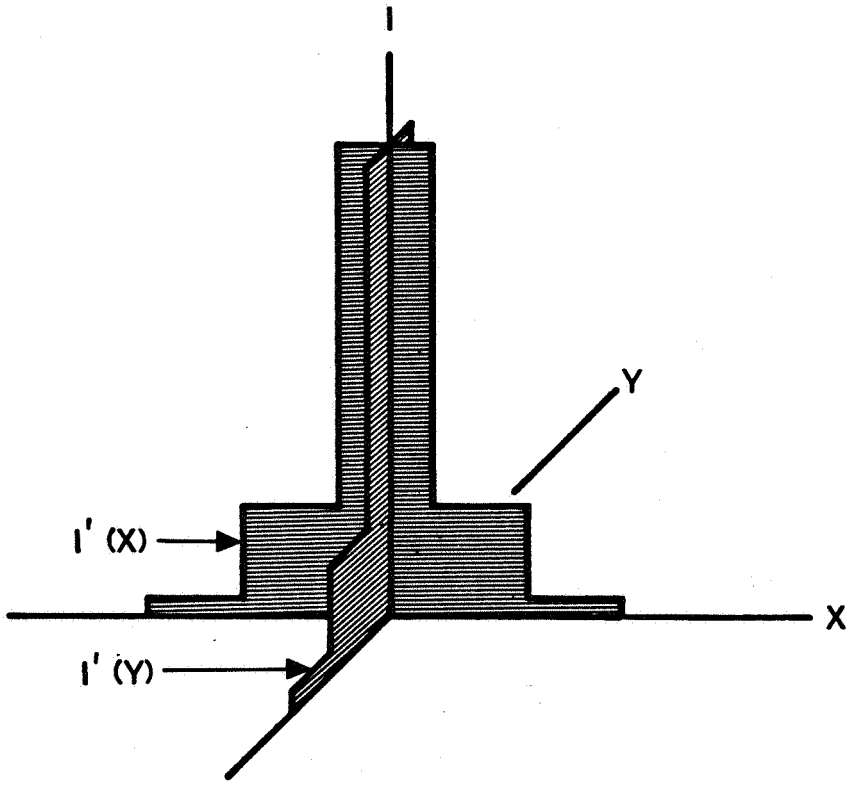

Figure 4. Image line spread functions as generated from CCD signals

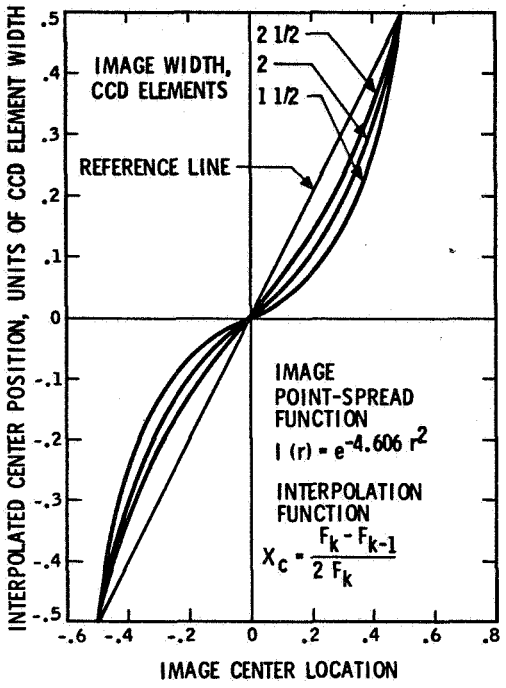

Figure 5. Interpolation of a Gaussian image by a vertical transfer CCD

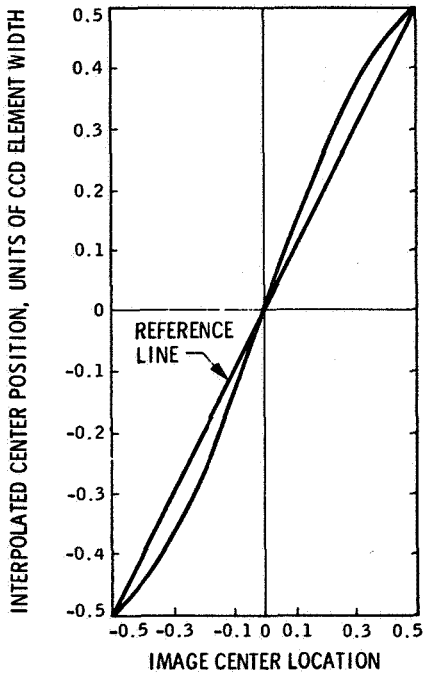

Figure 6. Interpolation of a Gaussian image by an interline transfer CCD